ELSEVIER

Polymer 42 (2001) 10133–10145

polymer

www.elsevier.com/locate/polymer

Thermophysical and mechanical properties of novel polymers prepared by the cationic copolymerization of fish oils, styrene and divinylbenzene

Fengkui Li, Annik Perrenoud, Richard C. Larock*

Department of Chemistry, Iowa State University, 2751 Gilman Hall, Ames, Iowa, IA 50011-3111, USA

Received 4 June 2001; received in revised form 7 August 2001; accepted 9 August 2001

Abstract

New polymeric materials have been prepared from the cationic copolymerization of fish oil ethyl ester (NFO), conjugated fish oil ethyl ester (CFO) or triglyceride fish oil (TFO) with styrene and divinylbenzene initiated by boron trifluoride diethyl etherate ($BF_3{\cdot}OEt_2$). These materials are typical thermosetting polymers with crosslink densities ranging from 1.1×10^2 to 2.5×10^3 mol/m^3. The thermogravimetric analysis of the new fish oil polymers exhibits three distinct decomposition stages at 200–340, 340–500 and >500°C, respectively, with the maximum weight loss rate at approximately 450°C. Single glass-transition temperatures of T_g = 30–109°C have been obtained for the fish oil polymers. As expected, these new polymeric materials exhibit tensile stress–strain behavior ranging from soft rubbers through ductile to relatively brittle plastics. The Young's modulus (E) of these materials varies from 2 to 870 MPa, the ultimate tensile strength (σ_b) varies from 0.4 to 42.6 MPa, and the percent elongation at break (ϵ_b) varies from 2 to 160%. The failure topography indicates typical fracture mechanisms of rigid thermosets, and the unique fibrillation on the fracture surface gives rise to relatively high mechanical properties for the corresponding NFO polymer. The new fish oil polymers not only exhibit thermophysical and mechanical properties comparable to petroleum-based rubbery materials and conventional plastics, but also possess more valuable properties, such as good damping and shape memory behavior, which most petroleum-based polymers do not possess, suggesting numerous, more promising applications of these novel fish oil-based polymeric materials.

Keywords: Fish oil; Alkenes; Cationic copolymerization

1. Introduction

Polymeric materials prepared from readily available, renewable and inexpensive natural resources, such as carbohydrates, starch and proteins, have become increasingly important. The advantages of these polymers are their low cost, ready availability from a renewable natural resource, and their possible biodegradability [1].

Fish oil is a biodegradable, renewable natural resource with a high degree of unsaturation. While most fish oil has been used for human and animal feed, it has also been used industrially to produce protective coatings, lubricants, sealants, inks and surfactants [2]. The high degree of unsaturation present in fish oil also makes it possible to polymerize or copolymerize the unsaturated oils and their fatty acids into useful polymers. Typically, the fish oil polymers that have been reported so far appear to be viscous polymerized oils. These polymerized oils are useful in varnishes, detergents, drying oils, plasticizers for polyvinyl chloride, fast-drying binders for paints, primers for steel and wooden surfaces, coatings for motor vehicles, etc. [3,4].

Recently, we have reported the direct conversion of fish oil ethyl ester (NFO) and conjugated NFO (CFO) into viable solid polymers by cationic copolymerization with divinylbenzene (DVB) initiated by boron trifluoride diethyl etherate (BFE) [5–8]. The resulting thermosetting polymers have room temperature moduli and glass-transition temperatures that are comparable to those of commercially available conventional plastics. However, the fish oil–DVB plastics obtained have very high crosslinking densities and non-uniform crosslinking structures, and thus appear to be very brittle, which significantly restricts their applications.

We have found that a combination of monofunctional styrene (ST) and difunctional DVB comonomers successfully reduces the non-uniformity of the crosslinking structure of the resulting fish oil polymers, like the corresponding soybean oil polymers we have reported previously [9–11]. As a result, the mechanical properties of the fish oil plastics have been significantly improved. In this work, we have obtained a variety of viable polymeric materials, ranging from elastomers through ductile to rigid plastics. These

* Corresponding author. Tel.: +1-515-294-4660; fax: +1-515-294-0105.
E-mail address: larock@iastate.edu (R.C. Larock).

0032-3861/01/$ - see front matter
PII: S0032-3861(01)00572-9

new fish oil–ST–DVB polymeric materials not only have thermal, physical and mechanical properties comparable to petroleum-based polymers, but also have even more promising and valuable properties, such as good damping properties and shape memory behavior, that most petroleum-based rubbers and plastics do not possess. This paper reports our systematic investigation of the thermophysical and mechanical properties of these new fish oil–ST–DVB polymers. The damping properties and shape memory behavior of the new polymers have also been investigated.

2. Experimental

2.1. Materials

The Norway fish oil ethyl ester (NFO) used in this study was Norwegian Pronova EPAX 5500 EE, Bergen, Norway. The conjugated NFO (CFO) was prepared from the NFO in our laboratory by using Wilkinson's catalyst [$RhCl(PPh_3)_3$] [12]. The degree of conjugation was calculated to be about 90 mol%. The triglyceride fish oil (TFO) is Norwegian Pronova EPAX 5500 TG, Bergen, Norway. Styrene and divinylbenzene (80 mol% DVB and 20 mol% ethylvinylbenzene) have been purchased from Aldrich Chemical Company and used as received. The distilled grade boron trifluoride diethyl etherate ($BF_3{\cdot}OEt_2$) used to initiate cationic polymerization of the various fish oils was also supplied by Aldrich.

2.2. Copolymerization

The polymeric materials have been prepared by the cationic copolymerization of NFO, CFO or TFO with ST and DVB initiated by BFE. The desired amounts of ST and DVB were added to the fish oil. The total amount of reactants was around 50 g. The reaction mixture was vigorously stirred, followed by the addition of an appropriate amount of BFE initiator. The reaction mixture was then injected into a Teflon mold, which was sealed by silicon adhesive and heated for a given time at the appropriate temperatures, usually 12 h at room temperature, followed by 12 h at 60°C and then 24 h at 110°C. The yields of resulting polymers are essentially quantitative. The nomenclature adopted in this work for the polymer samples is as follows: NFO, CFO and TFO represent fish oil ethyl ester, conjugated fish oil ethyl ester and triglyceride fish oil, respectively; ST and DVB are the styrene and divinylbenzene comonomers; BFE is the boron trifluoride diethyl etherate initiator. For example, NFO49–ST33–DVB15–BFE3 corresponds to a polymer sample prepared from 49 wt% NFO, 33 wt% ST, 15 wt% DVB and 3 wt% BFE initiator. Since the amount of ethylvinylbenzene present in the DVB is minimal, we have omitted it from our nomenclature to avoid confusion.

2.3. Characterizations

Soxhlet extraction was used to characterize the structures of the fish oil bulk polymers. A 2 g sample of the bulk polymer was extracted for 24 h with 100 ml of refluxing methylene chloride using a Soxhlet extractor. After extraction, the resulting solution was concentrated by rotary evaporation and subsequent vacuum drying. The soluble substances were isolated for further characterization. The insoluble solid was dried under vacuum for several hours before weighing.

A Perkin–Elmer Pyris-7 thermogravimeter was used to measure the weight loss of the polymeric materials in air. Generally, 6 mg of bulk polymer was used in the thermogravimetric analysis. The polymer samples were heated from 30 to 650°C at a heating rate of 20°C/min, and the weight loss was recorded as a function of temperature.

The dynamic mechanical properties of the bulk polymers were obtained by using a Perkin–Elmer dynamic mechanical analyzer DMA Pyris-7e in a three-point bending mode. The rectangular specimen was made by copolymerizing the reactants in an appropriate mold. Thin sheet specimens of 2 mm thickness and 5 mm depth were used, and the span to depth ratio was maintained at approximately 2. Each specimen was first cooled to ca −35°C, and then heated at 3°C/min and a frequency of 1 Hz under helium. The viscoelastic properties, i.e. storage modulus E', and mechanical loss factor (damping) tan δ, were recorded as a function of temperature. The glass-transition temperature T_g of the polymer was obtained from the peak of the loss factor curve.

The damping properties have been quantitatively evaluated by the loss tangent maximum $(\tan\delta)_{max}$, the temperature range ΔT for efficient damping ($\tan\delta > 0.3$), and the integral under the linear tan δ-temperature curve (tan δ area, TA). The TA values have been determined by first subtracting out the background, and then cutting and weighing the paper portions representing the tan δ area under consideration [13,14].

The shape memory behavior of the fish oil polymers was examined by a bending test [15]. The specimen (80 mm × 12 mm × 3 mm) was first deformed to a maximum angle θ_{max} at the temperature T_g + 50°C by an external force (the specimen tended to break at deformed angles greater than θ_{max}). The deformed specimen was then rapidly brought to ambient temperature under the external force. When the external force was released at room temperature, minor shape recovery may occur, and the deformed angle changes from θ_{max} to θ (the deformed angle θ fixed at room temperature is typically a little smaller than the originally deformed angle θ_{max}). Finally, the deformed specimen was heated to various temperatures rapidly, and the remaining angle θ_1 at each temperature was recorded. The following definitions are employed in order to quantitatively characterize the shape memory properties of the polymers. The deformability (D) of the specimen at the deformation temperature $T_D = T_g + 50$°C is defined as $D = \theta_{max}/180 \times 100\%$.

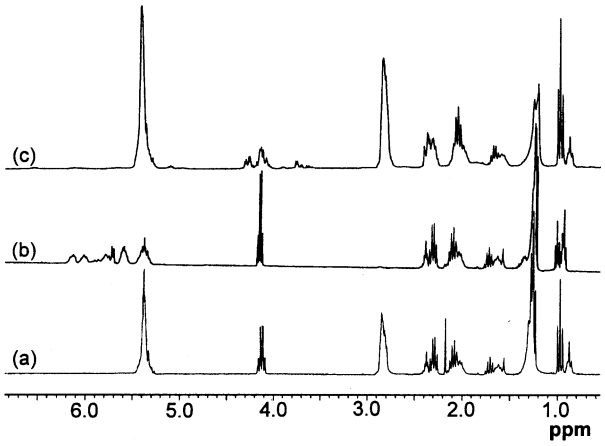

Fig. 1. ^{1}H NMR spectra of (a) NFO, (b) CFO and (c) TFO.

The fixed deformation (FD) at room temperature, which depicts the ability of the specimen to fix its deformation at room temperature, is defined as $FD = \theta/\theta_{max} \times 100\%$. The shape recovery is defined as $R = (\theta - \theta_1)/\theta \times 100\%$.

All of the ^{1}H NMR spectra were recorded in $CDCl_3$ using a Varian Unity spectrometer at 300 MHz.

The tensile tests have been conducted at 25°C according to ASTM-D638M specifications using an Instron universal testing machine (Model-4502) at a cross-head speed of 5 mm/min. The dumbbell-shaped test specimen has a gauge section with a length of 50 mm, a width of 10 mm, and a thickness of 3 mm. The gauge section is joined to wider end sections by two long tapered sections. The dumbbell-shaped specimens were prepared by cutting the material out of a polymer plate, and at least five identical specimens were tested for each polymer sample. The Young's modulus (E), ultimate tensile strength (σ_b) and elongation at break (ϵ_b) of the polymers were obtained from the tensile tests. The toughness of the polymer, which is the fracture energy per unit volume of the specimen, was obtained from the area under the corresponding tensile stress–strain curve.

Scanning electron microscopy (SEM) observations have been made using a Joel 5800LV SEM microscope. The failure surfaces of the test samples were carefully cut, and sputter-coated with palladium and gold, and then examined under the microscope.

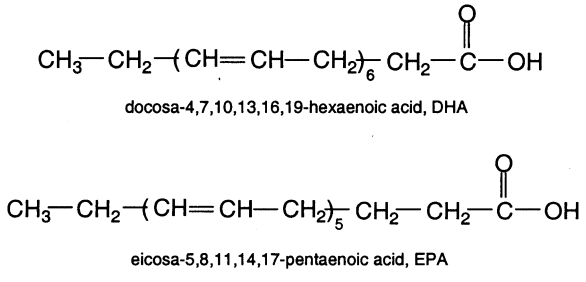

Fig. 2. Molecular structures of the fatty acids DHA and EPA in the fish oils.

3. Results and discussion

3.1. Structures of the fish oils, alkene comonomers, and their cationic copolymerization

The ^{1}H NMR spectra of the three fish oils used in this study are shown in Fig. 1. Fig. 1(a) indicates that the NFO used in this study is a mixture of fatty acid ethyl esters (the CH_2 of the ethyl esters is at $\delta = 4.0$–4.3 ppm) with a high degree of unsaturation (vinylic hydrogens at $\delta =$ 5.1–5.5 ppm). This oil is known to contain approximately 90 mol% of unsaturated fatty acid ethyl esters, more than 60 mol% of which have ≥5 non-conjugated C=C bonds [16]. The ^{1}H NMR spectrum of the conjugated NFO (CFO) in Fig. 1(b) indicates that conjugation does not affect the degree of unsaturation (vinylic hydrogens at $\delta =$ 5.1–6.5 ppm), and approximately 90 mol% of the C=C bonds that can be conjugated have been conjugated in the fatty acid ethyl esters. The ^{1}H NMR spectrum of the TFO in Fig. 1(c) clearly shows the protons in the methylene groups of the triglyceride at $\delta = 4.0$–4.4 ppm. The TFO is actually composed of 52 mol% triglyceride, 40 mol% diglyceride, 7 mol% monoglyceride and 1 mol% ethyl ester. Based on the spectra in Fig. 1, the NFO and CFO have been found to possess 3.6 C=C bonds per molecule on average, and the TFO has approximately 10 C=C bonds per triglyceride on average.

Fig. 2 shows the molecular structures of the two most abundant ω-3 fatty acids (esters) in the NFO and TFO, docosa-4,7,10,13,16,19-hexaenoic acid (DHA) and eicosa-5,8,11,14,17-pentaenoic acid (EPA). Accordingly, conjugated DHA and EPA, which are the major components of the CFO, exist as a number of fatty acid isomers, but the number of C=C bonds remains unchanged (not shown in Fig. 2).

The high degree of unsaturation of the three fish oils makes it possible to polymerize these oils by cationic polymerization. However, the viscous fish oils have relatively low mobility, and their reactivities are not high enough to give rise to high molecular weight polymers. Thus, alkene comonomers, such as ST and DVB, have to be added to get decent polymeric materials. These alkene comonomers possess lower molecular weights than the fish oils used. The conjugation of the C=C bonds with the aryl rings makes the ST and DVB more reactive towards cationic polymerization [17,18]. When the alkene comonomers are employed, viable solid polymeric materials have been obtained.

3.2. Microstructure of the fish oil polymers

A wide variety of viable polymeric materials ranging from soft rubbers to tough and rigid plastics have been prepared from cationic copolymerization of the fish oils and the alkene comonomers. The yields of the bulk polymers have been found to be essentially quantitative. These

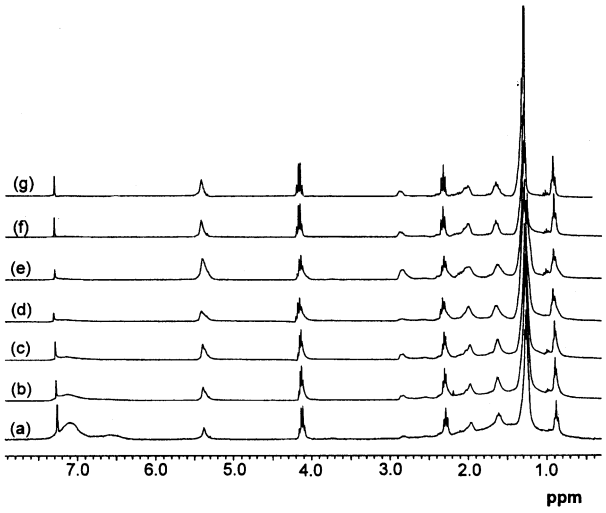

Fig. 3. ^{1}H NMR spectra of the soluble substances extracted from a number of NFO polymers NFO49 − (ST + DVB)48 − BFE3 with (a) 5 wt%, (b) 10 wt%, (c) 15 wt%, (d) 20 wt%, (e) 25 wt%, (f) 30 wt% and (g) 48 wt% DVB, respectively.

bulk materials are typical thermosetting polymers due to the multitude of C=C bonds present in the fish oils and the DVB comonomer. Soxhlet extraction using methylene chloride as the refluxing solvent was used to study the structure of the polymeric materials. Typically, after Soxhlet extraction for 24 h, about 56–88 wt% of insoluble substances are retained from the fish oil bulk polymers. These insoluble substances are found to be crosslinked fish oil–ST–DVB copolymers by solid state ^{13}C NMR spectroscopy [7]. The extracted soluble substances account for approximately 12–44 wt% of the bulk polymers. Fig. 3 shows the ^{1}H NMR spectra of the soluble substances extracted from a number of NFO-based bulk polymers. The spectra clearly show the presence of aromatic polymer segments $\delta = 6.5$–7.5 ppm as well as the NFO segments $\delta = 4.0$–4.3 ppm. These soluble substances appear to be mainly composed of fish oil–ST–DVB copolymers, but with relatively low molecular weights and less-crosslinked structures.

Table 1
Segmental compositions of the fish oil polymers

Entry	Polymer sample	Bulk polymer composition[a]	
		Insoluble part	Soluble part[b]
1	NFO30–ST46–DVB21–BFE3	88(22 + 66)	9(8 + 1)
2	NFO49–ST33–DVB15–BFE3	72(28 + 44)	25(21 + 4)
3	NFO60–ST25–DVB12–BFE3	56(24 + 32)	41(36 + 5)
4	NFO49–ST38–DVB10–BFE3	64(23 + 41)	33(26 + 7)
5	NFO49–ST33–DVB15–BFE3	72(28 + 44)	25(21 + 4)
6	NFO49–ST28–DVB20–BFE3	77(31 + 46)	20(18 + 2)
7	NFO49–ST23–DVB25–BFE3	78(31 + 47)	19(18 + 1)
8	NFO49–ST18–DVB30–BFE3	81(34 + 47)	16(15 + 1)
9	NFO49–ST00–DVB48–BFE3	86(38 + 48)	11(11 + 0)
10	NFO49–ST33–DVB15–BFE3	72(28 + 44)	25(21 + 4)
11	CFO49–ST33–DVB15–BFE3	85(38 + 47)	12(11 + 1)
12	TFO49–ST33–DVB15–BFE3	85(46 + 39)	12(3 + 9)

[a] Both the insoluble (crosslinked) and soluble (low molecular weight and less-crosslinked) substances by extraction in methylene chloride are composed of fish oil–ST–DVB copolymers. The result, for example 88 (22 + 66) in entry 1, means that insoluble crosslinked copolymer constitutes 88 wt% of the bulk polymer, of which approximately 22 wt% are polymerized fish oil segments and approximately 66 wt% are aromatic segments in the copolymer backbones.

[b] Since a minimal amount of initiator is incorporated into the polymer chains, about 3 wt% of initiator fragments should actually exist in the soluble substances. This amount of initiator residue has been subtracted from the soluble part in this table before calculation. Note that addition of the insoluble part and the soluble part plus 3 wt% initiator residue equals 100 wt%.

Table 1 lists the segment compositions of the fish oil polymers prepared in this study[1]. For all of the NFO polymers, the insoluble crosslinked NFO–ST–DVB copolymers contain greater amounts of rigid aromatic (ST + DVB) segments, whereas the soluble less-crosslinked fish oil–ST–DVB copolymers contain greater amounts of flexible polymerized fish oil segments in the polymer backbones (entries 1–9). An increase in NFO concentration does not obviously influence the polymerized NFO segments in the insoluble crosslinked copolymers, but significantly increases the amount of NFO segments in the soluble less-crosslinked copolymers (entries 1–3). On the other hand, with increasing DVB concentration, the wt% of the aromatic segments and fish oil polymer segments both gradually increase in the insoluble crosslinked copolymers (entries 4–9).

With the same composition, the resulting polymers based on different fish oils have different compositions in their copolymer backbones (entries 10–12). Compared with the NFO polymer (entry 10), the more reactive conjugated C=C bonds in the CFO result in greater amounts of fish oil segments being incorporated into the insoluble crosslinked copolymers, but the aromatic segments still dominate the composition (entry 11). The TFO has a triglyceride structure and approximately 10 C=C bonds, and thus essentially acts as a crosslinking agent like DVB. As a result, a greater amount of fish oil polymer segments than aromatic polymer segments has been obtained in the insoluble crosslinked polymer backbones (entry 12).

3.3. Thermogravimetric analysis

Fig. 4 shows the thermogravimetric analysis (TGA) curves and their derivatives for the NFO polymers prepared by varying the NFO concentrations. The thermosetting polymers appear to be relatively thermally stable at temperatures lower than 200°C. These materials lose

[1] The polymer segmental compositions have been estimated from the ^{1}H NMR spectra of the soluble substances and the stoichiometries by taking into account the fatty acid compositions of the fish oils and the quantitative yield of the cationic copolymerization. The soluble part is mainly composed of low molecular weight and less-crosslinked fish oil–ST–DVB copolymers, and may contain minimal unreacted free oils and initiator fragments.

Table 2
Characteristics of the fish oil polymers

Entry	Polymer sample	ν_e (mol m^{-3})	TGA results, °C (wt% loss)[a]			Damping results				Shape memory results (%)[c]		
			T_1	T_2	T_3	T_g (°C)	(tan δ)$_{max}$	ΔT[b]	TA	D	FD	R
1	NFO30–ST46–DVB21–BFE3	9.9×10^2	264(7.8)	467(84.4)	620(7.8)	109	0.94	87–137(50)	43	53	99	100
2	NFO49–ST33–DVB15–BFE3	3.7×10^2	247(20.9)	456(72.5)	610(6.6)	63	1.09	35–95(60)	59	85	97	100
3	NFO60–ST25–DVB12–BFE3	1.1×10^2	263(22.8)	455(71.6)	608(5.6)	30	2.07	− 8-78(86)	111	100	10	100
4	NFO49–ST38–DVB10–BFE3	1.2×10^2	260(22.8)	445(72.0)	605(5.2)	46	3.10	24–82(58)	95	95	90	100
5	NFO49–ST33–DVB15–BFE3	3.7×10^2	247(20.9)	456(72.5)	610(6.6)	63	1.09	35–95(60)	59	85	97	100
6	NFO49–ST28–DVB20–BFE3	5.7×10^2	250(20.7)	460(70.8)	620(8.5)	64	0.62	45–95(50)	44	71	98	100
7	NFO49–ST23–DVB25–BFE3	1.0×10^3	244(15.5)	460(76.1)	620(8.4)	88	0.44	69–115(46)	39	46	99	100
8	NFO49–ST18–DVB30–BFE3	1.5×10^3	220(12.7)	460(78.4)	605(8.9)	91	0.32	82–105(23)	33	22	100	100
9	NFO49–ST00–DVB48–BFE3	2.5×10^3	292(9.8)	474(76.7)	623(13.5)	105	0.14	0	15	6	100	100
10	NFO49–ST33–DVB15–BFE3	3.7×10^2	247(20.9)	456(72.5)	610(6.6)	63	1.09	35–95(60)	59	85	97	100
11	CFO49–ST33–DVB15–BFE3	1.1×10^3	260(11.9)	434(80.4)	560(7.7)	83	0.59	64–117(53)	38	50	99	100
12	TFO49–ST33–DVB15–BFE3	5.2×10^2	268(8.5)	455(83.9)	602(7.6)	88	1.53	66–118(52)	56	71	98	100

[a] The results outside the parentheses represent the temperatures at which the fastest weight loss rate occurs during the corresponding decomposition stage, and the results inside the parentheses represent the total weight loss during the corresponding decomposition stage.

[c] D is the deformability of the specimens at $T_g + 50$°C, FD is the percentage of fixed deformation at room temperature, and R is the final recovery of the fixed deformation.

[b] 24–82(58) means that the temperature ranges from 24 to 82°C at tan $\delta > 0.3$, and the $\Delta T = 58$°C.

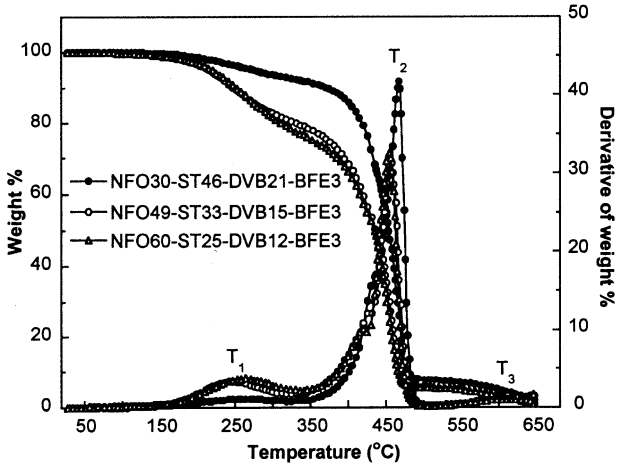

Fig. 4. TGA curves and their derivatives for the NFO polymers prepared by varying the NFO concentration.

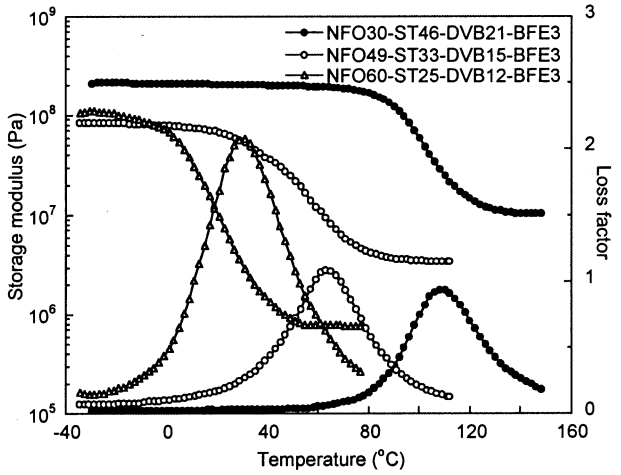

Fig. 5. Temperature dependence of the storage modulus and loss factor for the NFO polymers prepared by varying the NFO concentration.

about 8–23% of their weight at temperatures between 200 and 350°C, followed by an abrupt weight loss of 72–84% at temperatures between 350 and 500°C. The residual 10% weight loss occurs at $T > 500$°C. The wt% derivative curves clearly show the appearance of three decomposition stages at $T_1 = 200$–340°C, $T_2 = 340$–500°C, and $T_3 > 500$°C, respectively, with the maximum weight loss rate at T_2. Table 2 (entries 1–3) gives the TGA results for the NFO polymers. When the NFO concentration increases, the resulting NFO polymers exhibit an increased weight loss from 7.8 to 22.8% at T_1, an decreased weight loss from 84.4 to 71.6% at T_2, and an decreased weight loss from 7.8 to 5.6% at T_3. We have found that the weight losses at T_1 are inherently associated with the low molecular weight and less-crosslinked fish oil–ST–DVB copolymers in the bulk materials. The second stage (T_2) corresponds to degradation and char formation of the crosslinked polymer networks, and the third decomposition stage (T_3) corresponds to oxidation of the char residues in air [6,7].

The DVB concentration is also expected to affect the thermal properties of the resulting NFO polymers. An increase in DVB concentration obviously reduces the amounts of the soluble less-crosslinked copolymers in the resulting bulk materials (Table 1, entries 4–9). As a result, a gradual decrease in the weight loss at T_1 is observed in Table 2, entries 4–9. Greater amounts of DVB also result in an increase in crosslinking density, and thus increase the weight loss at T_2, and facilitate formation of residual chars at T_3 for the resulting polymers.

The thermal decomposition properties of the different fish oil-based polymers are also dependent upon their polymer compositions and crosslinking structures, even though they have the same original composition (Table 2, entries 10–12). When more reactive CFO replaces NFO, the wt% loss at T_1 significantly decreases, whereas the wt% loss at T_2 significantly increases. Although the conjugated C=C bonds in the CFO are expected to be more reactive than the non-conjugated C=C bonds in the TFO, the TFO has a higher number of C=C bonds, and its triglyceride structure essentially contributes more to crosslinking than the linear CFO. As a result, TFO polymer possesses higher thermal properties than either the NFO or the CFO polymer.

3.4. Dynamic mechanical behavior

Fig. 5 shows that the NFO polymers prepared by varying the NFO concentration exhibit dynamic mechanical behavior similar to one another. The storage modulus initially remains almost constant at lower temperatures. As the temperature increases, the storage modulus exhibits a sharp drop, followed by a modulus plateau at higher temperatures, where the polymer behaves like a rubber. Apparently, the modulus drop corresponds to the onset of segmental mobility in the crosslinked polymer networks. The appearance of a relatively constant modulus at higher temperatures indicates that stable crosslinked networks exist in the bulk polymer. The storage moduli of the NFO polymers are obviously related to the NFO concentrations in the polymer composition. As the NFO concentration increases, the resulting polymers show lower storage modulus over most of the temperature range studied. The onset of segmental mobility also shifts to lower temperatures. In addition, the rubbery moduli of the NFO polymers at $T > T_g$ are inherently associated with their degree of crosslinking. Based upon rubber elasticity theory [19,21], the crosslinking densities v_e of these three NFO polymers are calculated to be approximately 9.9×10^2, 3.7×10^2, and 1.1×10^2 mol/m^3 (Table 2, entries 1–3). The gradual decrease in crosslink densities is presumably due to the decreased amounts of crosslinking agent DVB in their compositions.

For each NFO polymer studied, a single loss factor peak has been observed. These loss factor peaks correspond to the glass-transition temperatures, i.e. α-relaxations of the crosslinked NFO polymers. As the NFO concentration increases,

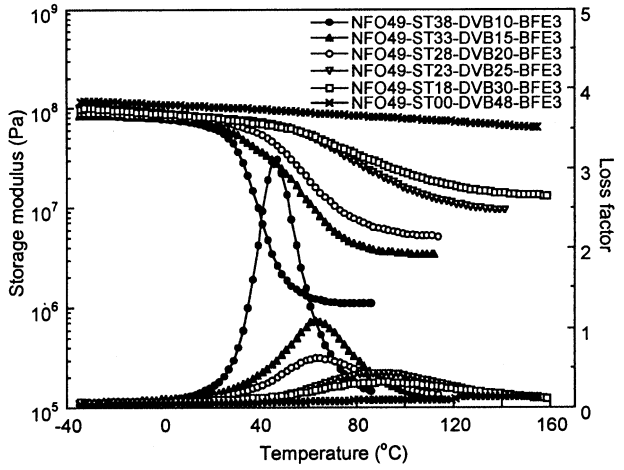

Fig. 6. Temperature dependence of the storage modulus and loss factor for the NFO polymers prepared by varying the DVB concentration.

the loss factor peaks of the resulting NFO polymers shift to lower temperatures from 109 to 30°C, and the loss factor becomes intense. The single α-relaxation indicates that the new NFO polymers obtained in this study exhibit a single homogeneous phase at the molecular level. The structures of these polymers are mainly composed of insoluble crosslinked NFO–ST–DVB copolymer matrix interpenetrated with some soluble low molecular weight and less-crosslinked NFO–ST–DVB copolymers. Apparently, these copolymers, although containing different segmental compositions as mentioned in Table 1, are thermodynamically miscible.

Fig. 6 shows the temperature dependence of the storage moduli E' and loss factors for NFO polymers prepared by varying the DVB concentration, while the total concentration of the comonomers ST plus DVB remains constant at 48 wt%. When less than 5 wt% DVB is used, the resulting polymers behave like a non-vulcanized rubber, which cannot be made into specimens suitable for DMA measurements. Viable polymeric materials have been obtained by employing at least 10 wt% DVB. The polymer NFO49–ST38–DVB10–BFE3 shows very low moduli, especially at high temperatures, and its loss factor shows a very sharp peak at about 46°C. An increase in the DVB concentration does not greatly affect the low temperature moduli of the resulting polymers, but their high temperature moduli exhibit a dramatic increase. Such behavior is expected, because increasing the DVB concentration obviously increases the degree of crosslinking. As the DVB concentration further increases, the molecular motions become more and more restricted, and thus the amount of energy that can be dissipated throughout the polymer specimen decreases dramatically. Therefore, the loss factor peak positions of the polymers shift to higher temperatures, and the loss factor intensities diminish accordingly. At an extremely high level of crosslinking, the tan δ peak almost disappears. As a result of crosslinking, a significant broadening of the α-relaxation is also observed. The broadening of the glass-to-rubber transition region is often assumed to be due to a broader distribution in molecular weight between crosslinks of some other kinds or heterogeneities in the network structure [20,22].

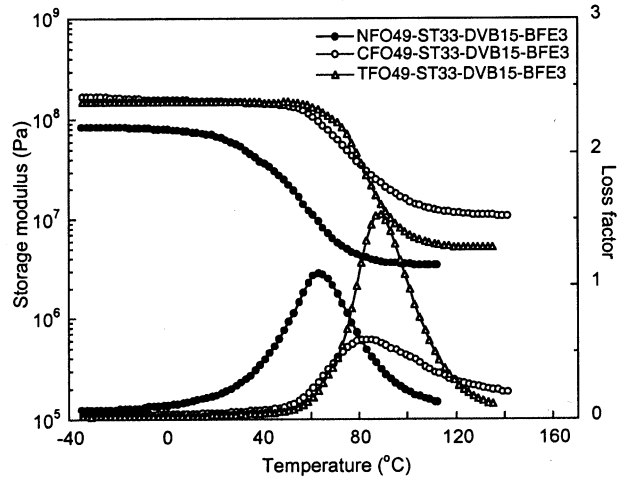

Fig. 7. Temperature dependence of the storage modulus and loss factor for NFO, CFO and TFO polymers with the same stoichiometry.

Fig. 7 gives the temperature dependence of the storage modulus E' and the loss factor for the NFO, CFO and TFO polymers with the same composition. Compared with the NFO, the CFO is more reactive due to its conjugated C=C bonds. Thus, the resulting CFO polymer CFO49–ST33–DVB15–BFE3 possesses higher storage moduli over the whole temperature region than the corresponding NFO polymer. The glass-transition temperatures also increase from 63 to 83°C. The triglyceride structure of the more highly unsaturatured TFO should contribute more to crosslinking than the ethyl esters of CFO. In fact, the TFO segments are much more flexible than the rigid aromatic segments in the corsslinked polymer networks. As a result, the TFO polymer with the same composition shows a lower rubbery modulus, i.e. a lower crosslinking density than the corresponding CFO polymer. However, their moduli at low temperatures are very similar to each other, and the glass-transition temperatures are of the same order of magnitude.

3.5. Good damping properties

These new fish oil polymers exhibit good damping properties. Based upon group contributions to damping [23,24], the presence of ester groups attached to the polymer backbones in our fish oil bulk polymers should greatly contribute to their damping intensities. On the other hand, crosslinking restricts segmental motion, and thus reduces the fish oil polymer's ability to dissipate sound or vibration mechanical energy into thermal energy, i.e. reduces damping intensities near the glass transition. In addition, crosslinking increases the segmental heterogeneities of the polymer backbone, and thus effectively broadens the glass-transition (damping)

regions of the fish oil polymers. With appropriate compositions and crosslinking densities, therefore, these new fish oil polymeric materials are capable of showing efficient damping over a wide temperature range. Good damping materials should exhibit a high loss factor ($\tan\delta > 0.3$) over a temperature range of at least 60–80°C [25].

The loss factor $\tan\delta$, which indicates the damping ability of the material, is the ratio of the mechanical dissipation energy to the storage energy. Thus, a high $\tan\delta$ value is essential for good damping materials. Table 2 (entries 1–3) shows that, as the NFO concentration is increased, the loss tangent maxima $(\tan\delta)_{max}$ of the resulting NFO polymers rises from 0.94 to 2.07. The polymer NFO30–ST46–DVB21–BFE3 exhibits efficient damping ($\tan\delta > 0.3$) over a temperature range of $\Delta T = 50$°C (entry 1). The damping of this polymer is improved by increasing the NFO concentration due presumably to the increasing number of ester groups in the resulting polymer backbone [23,24]. The polymers NFO49–ST33–DVB15–BFE3 and NFO60–ST25–DVB12–BFE3 show high damping ($\tan\delta > 0.3$) over much broader temperature ranges of $\Delta T = 60$°C and $\Delta T = 86$°C (entries 2 and 3), and are therefore also good damping materials. Their TA values reach 59 and 111, respectively, which are even higher than those of polyurethane-based IPN damping materials [26].

At a constant NFO concentration, the amounts of the crosslinking agent DVB obviously determine the crosslink densities, and thus significantly influence the damping properties of the resulting NFO polymers. As previously mentioned, at least 10 wt% DVB is required to afford a viable solid polymer material. The polymer NFO49–ST38–DVB10–BFE3 exhibits a $(\tan\delta)_{max}$ value as high as 3.1, a temperature region of $\Delta T = 58$°C at ($\tan\delta > 0.3$), and a high TA value of 95 K (entry 4). As the DVB concentration increases, the $(\tan\delta)_{max}$ and TA values of the resulting polymers gradually decrease. However, the ΔT value first increases, reaching a maximum at 15 wt% DVB, and then gradually decreases. Overall, when less than 15 wt% DVB is employed, the resulting polymers exhibit high damping ($\tan\delta > 0.3$) over a wide temperature range ($\Delta T = 58$–60°C) (entries 4 and 5). When 20–25 wt% DVB is used, the resulting NFO polymers still show a relatively broad temperature range for efficient damping ($\Delta T = 46$–50°C) (entries 6 and 7). However, when more than 30 wt% DVB is employed, the resulting polymers exhibit $(\tan\delta)_{max}$ values in the vicinity or much lower than 0.3, and are no longer good damping materials (entries 8 and 9).

The damping results for polymers based on different fish oils are also listed in Table 2, entries 10–12. The polymer NFO49–ST33–DVB15–BFE3 is a good damping material (entry 10). The high reactivity of the conjugated NFO (CFO) results in a high crosslink density, and the reduction of damping intensity by crosslinking becomes pronounced. As a result, the damping properties of the CFO polymers are inferior to those of the corresponding NFO polymer. As mentioned above, the triglyceride TFO is likely to contribute more to crosslinking of the polymer backbones. The relatively greater amounts of ester groups incorporated into the TFO polymer backbones give rise to the highest $(\tan\delta)_{max}$ value of the three different fish oil polymers.

3.6. Thermally stimulated shape memory behavior

Shape memory refers to the ability of certain materials to remember a shape, on demand, even after rather severe deformations [27]. The basic principle of the shape memory effect in polymeric materials can be well described by their elastic modulus-temperature behavior. At temperatures above the glass-transition temperature (T_g), the polymer achieves a rubbery elastic state where it can be easily deformed. When the material is then cooled below its T_g, the deformation is fixed and the deformed shape is obtained. The deformed material can easily return to its original shape by reheating the material to a temperature higher than the T_g. Therefore, there are two prerequisites for a polymer to exhibit a shape memory effect. One is that the material's T_g should be higher than ambient temperature, and the other is that a stable crosslinked polymer network should exist in the bulk polymer [28,29].

As previously mentioned, most of the fish oil polymers possess glass-transition temperatures higher than room temperature (Table 2), and stable crosslinked polymer networks have been shown to exist in the bulk materials. Thus, the fish oil polymers are expected to show shape memory effect. The shape memory results of the fish oil polymers are also included in Table 2. The NFO polymer NFO30–ST46–DVB21–BFE3 has a relatively low deformability at $T > T_g$ ($D = 53\%$), but exhibits a good ability to fix its deformation (FD = 99%) at room temperature (entry 1). As the NFO concentration is increased, the resulting polymer shows an improved deformability ($D = 85\%$) at $T > T_g$, but its ability to fix the deformation is reduced to FD = 97% (entry 2). When the NFO concentration exceeds 50 wt%, the resulting polymer actually shows characteristics of an elastomer with FD = 10% (entry 3). As expected, the DVB concentration has an effect on the shape memory behavior of the resulting NFO polymers contrary to that of the NFO concentration. Typically, an increase in DVB concentration reduces the deformability of the resulting NFO polymers at $T > T_g$, but improves the ability of the polymers to fix their deformation at ambient temperature (entries 4–9). It follows that the deformability of the polymer at $T > T_g$ is determined by the rubbery modulus at high temperatures, whereas the ability of the polymer to fix its deformation at room temperature is determined by the room temperature modulus. The driving force for shape recovery of the deformed fish oil polymers is the strong relaxations of the oriented polymer chains between crosslinks, which occurs during heating above the glass-transition temperature. Note that all of the polymers show 100% recovery of the fixed deformation upon reheating to $T_g + 50$°C, indicating

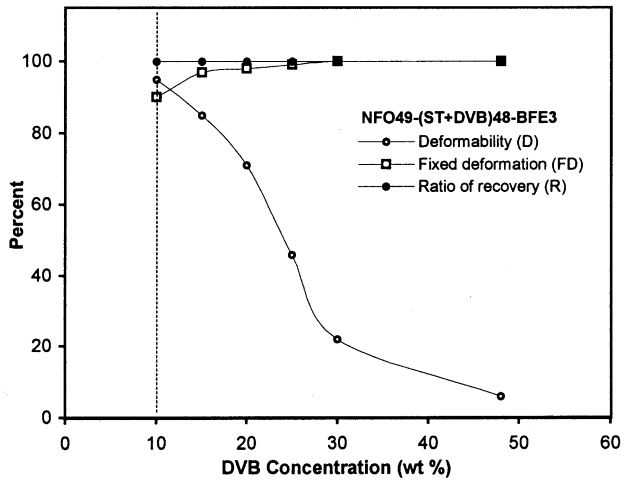

Fig. 8. Plots of shape memory results versus DVB composition in the fish oil polymers.

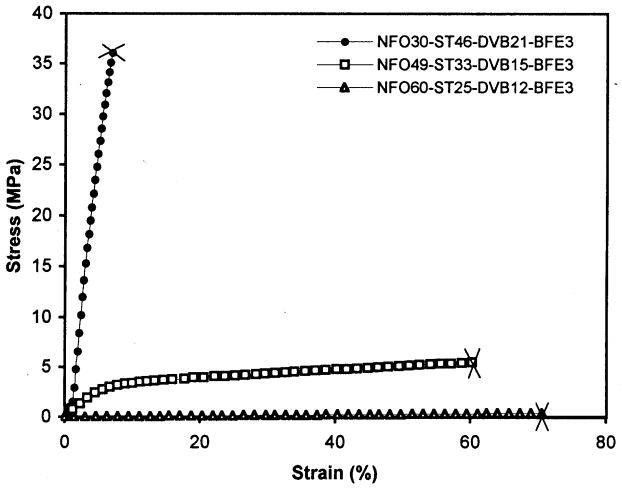

Fig. 10. Tensile stress-strain curves for the NFO polymers prepared by varying the NFO concentration.

that the crosslink density is high enough to effectively store and release the stored elastic energy at various temperatures. Fig. 8 shows the plot of shape memory results versus the DVB concentration. The optimal combinations of shape memory properties are found in two NFO polymers NFO49–ST38–DVB10–BFE3 and NFO49–ST33–DVB15–BFE3 (Table 2; entries 4 and 5). Their properties are very close to those of the petroleum-based shape-memory polymers with deliberately designed molecular structures, such as grafted copolymers [30], segmented block copolymers [15,28,29,31,32], and some hybrid copolymers [27]. In addition, the polymers based on different fish oils show similar abilities to fix deformation at ambient temperature (entries 10–12), although their deformabilities are different from one another. Overall, the NFO polymer exhibits better shape memory properties than the corresponding CFO and TFO polymers.

Fig. 9 shows the shape recovery results at various temperatures for two NFO polymers. The polymer NFO49–ST38–DVB10–BFE3 shows an onset of shape recovery at low temperatures; 100% recovery is reached at about 60°C. The NFO49–ST33–DVB15–BFE3 shows an onset of shape recovery at relatively high temperatures, and full shape recovery is obtained at about 80°C. These initial shape recovery processes are inherently related to the onset of segmental motions (glass transition) in the NFO polymers. Due to the broad glass transitions (damping), the shape recovery temperature ranges for the two NFO polymers are also very broad, i.e. 40–50°C.

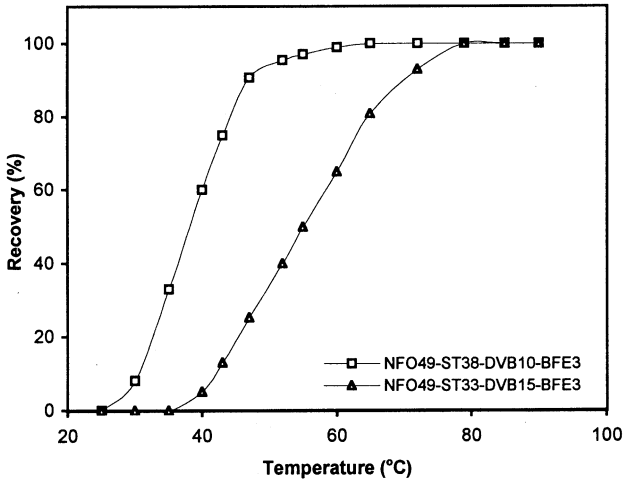

Fig. 9. The shape recovery rates of the NFO polymers as a function of temperature.

3.7. Tensile mechanical properties

Fig. 10 shows the tensile stress–strain behavior of the NFO polymers prepared by varying the NFO concentration, while the weight ratio of ST to DVB comonomers remains at approximately 2:1. The tensile behavior of the polymers is highly dependent upon the NFO concentration. For example, the polymer NFO30–ST46–DVB21–BFE3 has a composition with rigid aromatic comonomers prevalent in the stoichiometry. This polymer shows the typical tensile behavior of a rigid plastic with a Young's modulus E of 870 MPa, an ultimate tensile strength σ_b of 36.1 MPa, and an elongation at break ϵ_b of about 7% (Table 3, entry 1). As the NFO concentration increases and the NFO becomes equivalent to the ST plus DVB comonomers in weight, the resulting polymer NFO49–ST33–DVB15–BFE3 shows the typical stress–strain behavior of a soft plastic. Compared with the rigid plastic NFO30–ST46–DVB21–BFE3, the soft plastic NFO49–ST33–DVB15–BFE3 shows a big decrease in the Young's modulus E and ultimate tensile strength σ_b, but a significant increase in the ductility and toughness (entry 2). As the NFO concentration exceeds that of the comonomers, the resulting polymer NFO60–ST25–DVB12–BFE3 exhibits tensile behavior similar to a very soft rubbery material (entry 3).

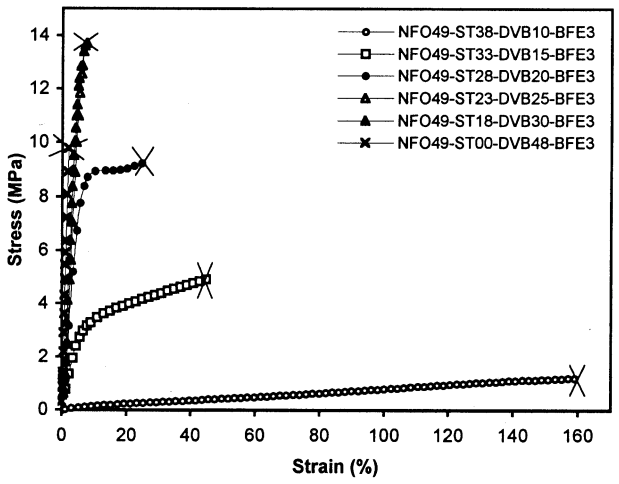

Fig. 11. Tensile stress–strain curves for the NFO polymers prepared by varying the DVB concentration.

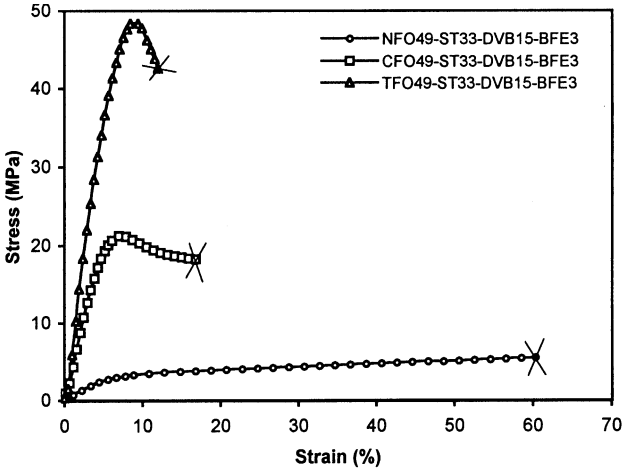

Fig. 12. Tensile stress–strain curves for NFO, CFO and TFO polymers with the same stoichiometry.

Fig. 11 shows the room temperature tensile behavior of the NFO polymers prepared by varying the DVB concentration. The polymers NFO49–ST48–DVB00–BFE3 and NFO49–ST43–DVB05–BFE3 appear to be non-vulcanized rubbers without elasticity, and cannot be made into specimens suitable for tensile tests at room temperature. When 10 wt% of DVB is employed, the resulting polymer NFO49–ST38–DVB10–BFE3 shows a rubbery modulus, a viable ultimate tensile strength σ_b and an elongation at break ϵ_b of approximately 160% (Table 3, entry 4). Even though its glass-transition temperature T_g (46°C) is a little higher than room temperature, this polymer exhibits tensile test behavior similar to a vulcanized natural rubber. When further increasing the amount of DVB, the Young's modulus E and ultimate tensile strength σ_b of the resulting polymers obviously increase, but their elongation at break ϵ_b gradually decreases (entries 5–8). When DVB has completely replaced the ST, the polymer NFO49–ST00–DVB48–BFE3 possesses the highest elastic modulus, but its ultimate tensile strength σ_b and elongation at break ϵ_b are considerably reduced (entry 9). The toughness of NFO polymer first increases with an increase in DVB concentration. It reaches a maximum at 15 wt% DVB (entry 5) and then gradually decreases. A very brittle NFO plastic with rather low toughness is obtained when pure DVB is employed (entry 9).

Fig. 12 shows the tensile stress–strain behavior of different fish oil polymers with the same composition. The NFO polymer exhibits characteristics of a soft plastic (Table 3, entry 10). The more reactive CFO results in a relatively hard plastic (entry 11), which shows the appearance of yielding behavior, followed by strain softening. No strain hardening behavior is observed before the specimen breaks. A very rigid plastic is obtained from the TFO. Its Young's modulus E reaches 820 MPa, and its ultimate tensile strength σ_b reaches 42.6 MPa (entry 12). The TFO plastic specimen breaks on the verge of its intrinsic yielding point.

Fig. 13 plots the Young's modulus E, ultimate tensile strength σ_b and elongation at break ϵ_b against crosslink densities ν_e of the NFO polymers prepared in this study. It shows that crosslinking dramatically affects the mechanical properties of the thermosetting polymers. Generally, the polymer segmental motions are frozen in a glassy state.

Table 3
Tensile mechanical properties of the fish oil polymers

Entry	Polymer sample	Young's modulus (MPa)	Tensile strength (MPa)	Elongation at break (%)	Toughness (MPa)
1	NFO30–ST46–DVB21–BFE3	870	36.1	6.9	1.21
2	NFO49–ST33–DVB15–BFE3	80	5.5	60.3	2.50
3	NFO60–ST25–DVB12–BFE3	2	0.4	70.6	0.15
4	NFO49–ST38–DVB10–BFE3	6	1.2	160.1	0.91
5	NFO49–ST33–DVB15–BFE3	80	5.5	60.3	2.50
6	NFO49–ST28–DVB20–BFE3	214	9.3	26.1	2.23
7	NFO49–ST23–DVB25–BFE3	359	14.6	10.3	0.99
8	NFO49–ST18–DVB30–BFE3	393	13.7	7.5	0.63
9	NFO49–ST00–DVB48–BFE3	537	9.8	2.0	0.14
10	NFO49–ST33–DVB15–BFE3	80	5.5	60.3	2.50
11	CFO49–ST33–DVB15–BFE3	450	18.3	16.8	2.44
12	TFO49–ST33–DVB15–BFE3	820	42.6	12.0	3.56

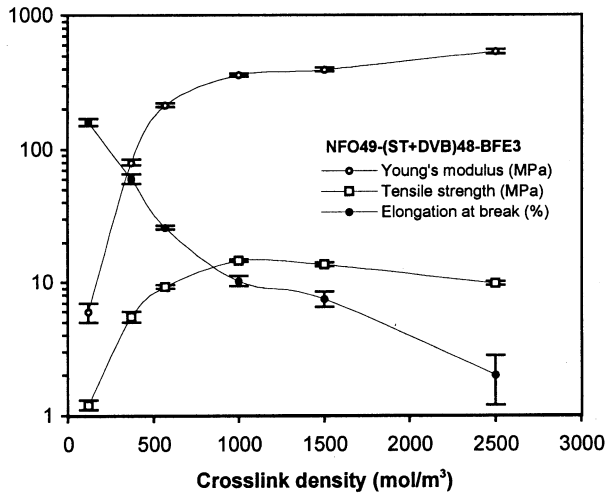

Fig. 13. Plots of Young's modulus (E), ultimate tensile strength (σ_b) and elongation at break (ϵ_b) against crosslink densities (ν_e) for the fish oil polymers.

The elastic modulus is obtained from the initial strain resulting from changes in the covalent bond lengths and angles generated upon loading. Thus, crosslinking has relatively little effect on the magnitude of the elastic modulus of the thermosetting polymers in the glassy state (i.e. at temperatures below their glass-transition temperatures) [20]. However, the room temperature Young's moduli of the new fish oil polymers shown in Fig. 13 have been greatly influenced by the degree of crosslinking, even though most of the materials possess a T_g higher than room temperature (refer to Table 2). However, it should be noted that the glass-transition regions of the fish oil polymers cover a wide temperature range, apparently including room temperature. This means that these glassy polymers contain frozen-in segmental chains, as well as mobile segmental chains. The change in covalent bond length and segmental deformations both contribute to the elastic behavior of the polymers. The segmental deformation, which is determined by the crosslinking density, is of course expected to make a major contribution. Thus, the Young's modulus of the fish oil polymers at room temperature is greatly affected by the degree of crosslinking.

In addition, crosslinking increases the number of bonding chains at a crack tip, and thus improves the ultimate tensile strength σ_b of the fish oil polymers (Fig. 13). However, when further increasing the crosslink density ν_e, the ultimate tensile strength σ_b of the polymers slightly decreases. It is speculated that high crosslinking reduces the number of conformations that the polymer can adopt upon being loaded. As a crack grows to a failure, the matrix can dissipate only a small amount of energy, leading to low ultimate tensile strength σ_b. Fig. 14 also shows a steady decrease in elongation at break ϵ_b with increasing crosslink density ν_e. Such behavior is expected, because crosslinking reduces the segmental mobility and flexibility of the polymer chains.

3.8. Failure topography and fracture mechanisms

Fig. 14 shows the SEM photograph of the tensile fracture surface of the rigid NFO plastic NFO30–ST46–DVB21–BFE3. Apparently, the fracture is initiated by a flaw, which normally is due to a material defect (flaw), such as a pore, an inclusion or any other local inhomogeneity [33]. A slow-growth mirror region, an area with a smooth, glossy appearance, surrounds the flaw region. Although rigid thermosets can and often exhibit plastic deformation under conditions of fracture [34], this is the first time, to our knowledge, that plastic deformations result in a thin layer of broken polymer

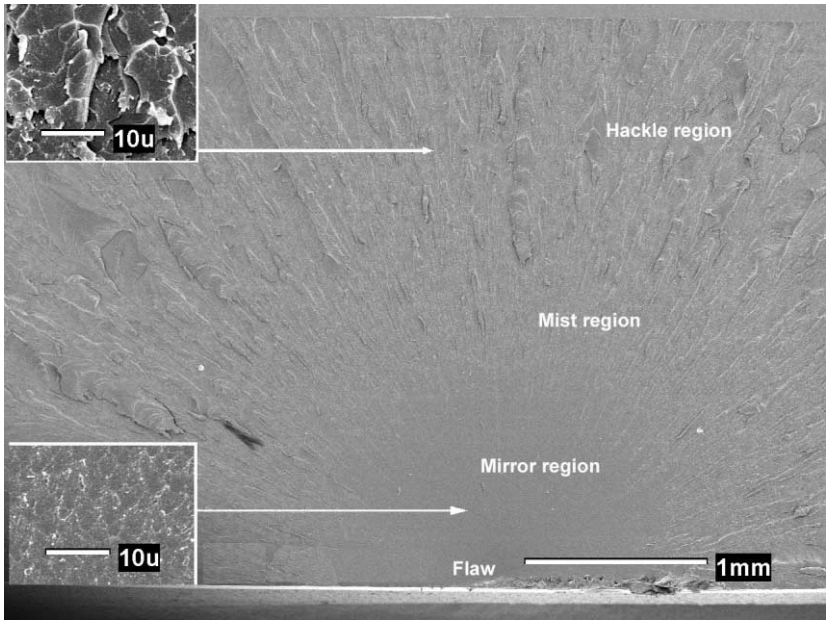

Fig. 14. SEM photograph of the fracture surface of the rigid plastic NFO30–ST46–DVB21–BFE3.

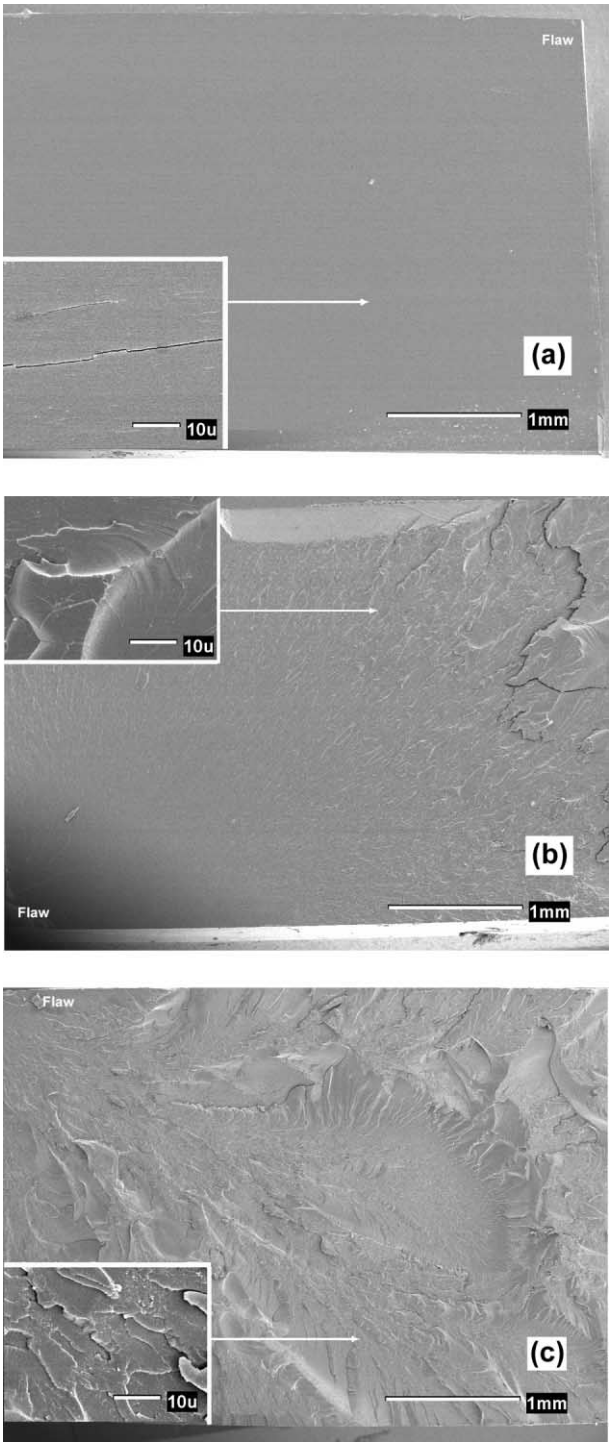

Fig. 15. SEM photographs of the fracture surfaces of (a) NFO, (b) CFO and (c) TFO plastics with the same stoichiometry (OIL49–ST33–DVB15–BFE3).

fibrils in the glossy mirror region. This particular plastic deformation behavior results in high mechanical properties for the NFO plastic (Table 3, entry 1). Rapid-growth mist and hackle regions cover the remainder of the surface, which shows a ridged and furrowed structure running parallel to the propagation direction. The direction of crack growth can be determined from river markings in the slow-growth region, which radiate from the point where the crack is initiated.

Fig. 15 shows the tensile fracture surfaces of the NFO, CFO, and TFO plastics with the same composition. Their fracture morphologies are consistent with their mechanical properties. For example, the polymer NFO49–ST33–DVB15–BFE3 has the lowest Young's modulus E and ultimate tensile strength σ_b (Table 3, entry 10), and a smooth fracture surface is observed even at high magnification. Comparatively, the CFO49–ST33–DVB15–BFE3 has a higher Young's modulus E and ultimate tensile strength σ_b (entry 11). Accordingly, mirror, mist and hackle regions all are observed on the fracture surface, and the fracture surface becomes increasingly rough along the crack propagation. The polymer TFO49–ST33–DVB15–BFE3 has a much higher Young's modulus E and ultimate tensile strength σ_b (Table 3, entry 12). Its whole fracture surface is rather rough. No single fracture mechanism is expected.

4. Conclusion

A variety of new polymeric materials ranging from elastomers through ductile to rigid plastics have been prepared from the cationic copolymerization of NFO, CFO or TFO with ST and DVB initiated by BFE. These thermosetting polymers possess crosslink densities ranging from 1.1×10^2 to 2.5×10^3 mol/m^3, and glass-transition temperatures ranging from 30 to 109°C. Although the materials are composed of fish oil–ST–DVB copolymers with various segmental compositions, all of the components are thermodynamically miscible in a single phase. The new polymers appear to be thermally stable at temperatures lower than 200°C. A multiple thermal decomposition behavior is observed with the maximum weight loss rate at approximately 450°C, which is inherently associated with the compositions and structures of the bulk polymers.

The tensile stress–strain behavior of the new fish oil polymers have been investigated as a function of their stoichiometry and the type of fish oil employed. The resulting polymers demonstrate a range of tensile behavior from soft rubbery materials through ductile to rigid plastics. Yielding behavior is observed in the tensile stress–strain curves of the CFO and TFO plastics. The TFO polymer possesses the highest mechanical properties, with the roughest fracture surfaces, compared to the corresponding NFO and CFO polymers.

In addition to thermophysical and mechanical properties comparable to petroleum polymers, the new fish oil polymers with appropriate compositions exhibit good damping properties and typical shape memory effects. These new and more promising properties make it possible to fabricate novel, value-added polymer products from these fish oil polymeric materials.

Acknowledgements

The authors are grateful to the Iowa Soybean Promotion Board for financial support. We also thank Dr J. Jane of the Food Science and Human Nutrition Department and Dr V. Sheares of the Chemistry Department at Iowa State University for use of their equipment.

References

[1] Kaplan DL. Biopolymers from renewable resoureces. New York: Springer, 1998.
[2] Fineberg H, Johanson AG. Industrial use of fish oils. In: Stansby ME, editor. Fish oils: their chemistry, technology, stability, nutritional properties, and uses, Connecticut: The AVI Publishing Company Inc, 1976. p. 222–38.
[3] Shigeno Y, Komori S, Yamamoto H. Chem Soc Jpn (Ind Chem Sect) 1998;59:63–67.
[4] DeSesa RJ. Uses in protective coatings. In: Stansby ME, editor. Fish oils: their chemistry, technology, stability, nutritional properties, and uses. Connecticut: The AVI Publishing Company, Inc, 1967. p. 246–9.
[5] Marks DW, Li F, Pacha CM, Larock RC. J Appl Polym Sci 2001;81(8):2001–12.
[6] Li F, Marks DW, Larock RC, Otaigbe JU. SPE ANTEC Tech Pap 1999;3:3821–5.
[7] Li F, Marks DW, Larock RC, Otaigbe JU. Polymer 2000;41(22):7925–39.
[8] Li F, Larock RC, Otaigbe JU. Polymer 2000;41(13):4849–62.
[9] Li F, Hanson MV, Larock RC. Polymer 2001;42(4):1567–79.
[10] Li F, Larock RC. J Polym Sci, Part B: Polym Phys 2000;38(21): 2721–38.
[11] Li F, Larock RC. J Polym Sci, Part B: Polym Phys 2001;39(1):60–77.
[12] Marks DW, Larock RC. Submitted for publication, 2001.
[13] Hu R, Dimonie VL, El-Aasser MS, Pearson RA, Hilner A, Mylonakis SG, Sperling LH. J Polym Sci, Part B: Polym Phys 1997; 35(10):1501–14.
[14] Fay JJ, Murphy CJ, Thomas DA, Sperling LH. Polym Eng Sci 1991;31(24):1731–41.
[15] Lin JR, Chen CW. J Appl Polym Sci 1998;69(8):1563–86.
[16] Technology International Exchange Inc., Certificate of Analysis for Pronova Fish Oil, Pronova, Biocare, 1996.
[17] Matyjaszewski K, editor. Cationic polymerizations: mechanisms, synthesis and applications. New York: Marcel Dekker, 1996.
[18] Kennedy JP, Marechal E. Carbocationic polymerization. New York: Wiley, 1982.
[19] Flory JP. Principles of polymer chemistry. Ithaca: Cornell University Press, 1953 chapter 6.
[20] Nielsen LE, Landel RF. Mechanical properties of polymers and composites. 2nd ed. New York: Marcel Dekker, 1994 chapter 4.
[21] Muruyama T. Dynamic mechanical analysis of polymeric materials. Amsterdam: Elsevier, 1978.
[22] Ferry JD. Viscoelastic properties of polymers. New York: Wiley, 1961.
[23] Chang MCO, Thomas DA, Sperling LH. J Polym Sci, Part B: Polym Phys 1988;26(8):1627–40.
[24] Corsaro RD, Sperling LH. Sound and vibration damping with polymers. ACS Symposium Series, No. 424. Washington DC: American Chemical Society, 1990.
[25] Yak S. In: Klemper D, Frisch KC, editors. Advances in interpreting polymer networks, vol. 4. Lancaster, PA: Technomic Publishing Company, 1994.
[26] Chern YC, Tseng SM, Hsieh KH. J Appl Polym Sci 1999;74(2):328–35.
[27] Jeon HG, Mather PT, Haddad TS. Polym Int 2000;49(5):453–7.
[28] Li F, Zhang X, Hou J, Xu M, Ma D, Luo X, Kim BK. J Appl Polym Sci 1997;64(8):1511–6.
[29] Takahashi T, Hayashi N, Hayashi S. J Appl Polym Sci 1996;60(7):1061–9.
[30] Li F, Chen Y, Zhu W, Zhang X, Xu M. Polymer 1998;39(26):6929–34.
[31] Kim BK, Lee SY, Xu M. Polymer 1996;37(26):5781–93.
[32] Skakalova V, Lukes V, Breza M. Macromol Chem Phys 1997;198(10):3161–72.
[33] Plangsangmas L, Mecholsky Jr. JJ, Brennan AB. J Appl Polym Sci 1999;72(2):257–68.
[34] Robertson RE, Mindroiu VE. Polym Eng Sci 1987;27(1):55–62.